

Iron-intercalated Zirconium Diselenide Thin Films from the Low Pressure Chemical Vapor Deposition of $[\text{Fe}(\eta^5\text{-C}_5\text{H}_4\text{Se})_2\text{Zr}(\eta^5\text{-C}_5\text{H}_5)_2]_2$

Clara Sanchez-Perez,^{†,‡} Caroline E. Knapp,[†] Ross H. Colman,[§] Carlos Sotelo-Vazquez,[†]

Sanjayan Sathasivam,[†] Raija Oilunkaniemi,[‡] Risto S. Laitinen,^{,‡} and Claire J. Carmalt^{*,†}*

Rietveld refinements were performed using GSAS and EXPGUI.^{1,2} All phases were modelled using a Pseudo-Voigt peak shape, GSAS profile function type 2. The large background contribution from Fe-fluorescence and an amorphous content from partially decomposed air-sensitive material was modelled using a shifted Chebyshev function with 20 terms. Preferred orientation of the highly 2-dimensional target compounds, Fe_xZrSe_2 , was observed and modelled using a 4th order spherical harmonic model resulting in a texture index 1.0104. Correlations between the preferred orientation parameters and the refined Fe occupancy within the Fe_xZrSe_2 structures suggests the estimated errors associated with the refined occupancies are underestimated. The data was not of suitable quality for refinement of Se occupancies relative to the Zr, a key feature that has previously been shown to alter both lattice parameters and electronic properties.^{3,4} The multiphase nature of the sample makes bulk elemental analysis to determine the Fe intercalant composition impossible.

Due to partial oxidation of the Fe_xZrSe_2 samples a significant contribution from ZrO_2 was observed. No Se was observed in our diffraction patterns likely due to a lack of crystallinity, adding to the observed amorphous background. Whilst zirconia, ZrO_2 , typically shows a monoclinic structure at room temperature, the incorporation of Fe has previously been shown to stabilise the cubic form, $c\text{-ZrO}_2$, at room temperature.⁵ The low crystallinity of these decomposition products results in extreme broadening of their associated diffraction peaks and so ZrO_2 , where only broad and ill-defined features are observed, the contributions were modelled using their cubic structures to minimise the number of free refinement parameters. Besides lattice parameters, no structural details were refined for the impurity phases and thermal parameters were fixed at a reasonable value.

The observation of $\gamma(\text{FCC})\text{-Fe}$ at room-temperature in bulk form is not expected and worth commenting on. It has previously been studied as a stabilised phase in epitaxially grown films on $\text{Cu}(001)$ and diamond surfaces.^{6,7,8} Lattice matching to the substrate (e.g. $\text{FCC-Fe } a \sim 3.59 \text{ \AA}$, $\text{Cu}(001) a = 3.61 \text{ \AA}$, diamond $a = 3.57 \text{ \AA}$) stabilises the FCC structure and so its appearance on Fe_xZrSe_2 ($a = 3.77 \text{ \AA}$) is not entirely unexpected here.

Table S1. Refined parameters for Fe_xZrSe_2 . The refinement quality of fit parameters χ^2 , R_{wp} and R_p are 8.443, 1.47 % and 1.10 %, respectively.

Phase	Space-group	a (Å)	b (Å)	c (Å)	β (°)	Phase fraction (wt. %)
	Atom	x/a	y/b	z/c	Occ	U_{iso} (Å ²)
Fe_xZrSe_2	$P-3m1$	3.77239(6)	3.77239(6)	6.1336(3)	120	61.9(10)
	Zr	0	0	0	1.0	0.0233(13)
	Se	1/3	2/3	0.2616(6)	1.0	0.008(4)
	Fe	0	0	0.5	0.135(5)	0.025
FeSe	$P6_3/mmc$	3.6962(12)	3.6962(12)	5.999(3)	120	9.11(12)
	Fe	0	0	0	1	0.025
	Se	1/3	2/3	1/4	1	0.025
α -Fe	$Im-3m$	2.87086(17)	2.87086(17)	2.87086(17)	90	3.55(6)
	Fe	0	0	0	1	0.025
γ -Fe	$Fm-3m$	3.6116(3)	3.6116(3)	3.6116(3)	90	5.18(9)
	Fe	0	0	0	1	0.025
ZrO_2	$Fm-3m$	5.1234(13)	5.1234(13)	5.1234(13)	90	20.25(19)
	Zr	0	0	0	1	0.025
	O	1/4	1/4	1/4	1	0.025

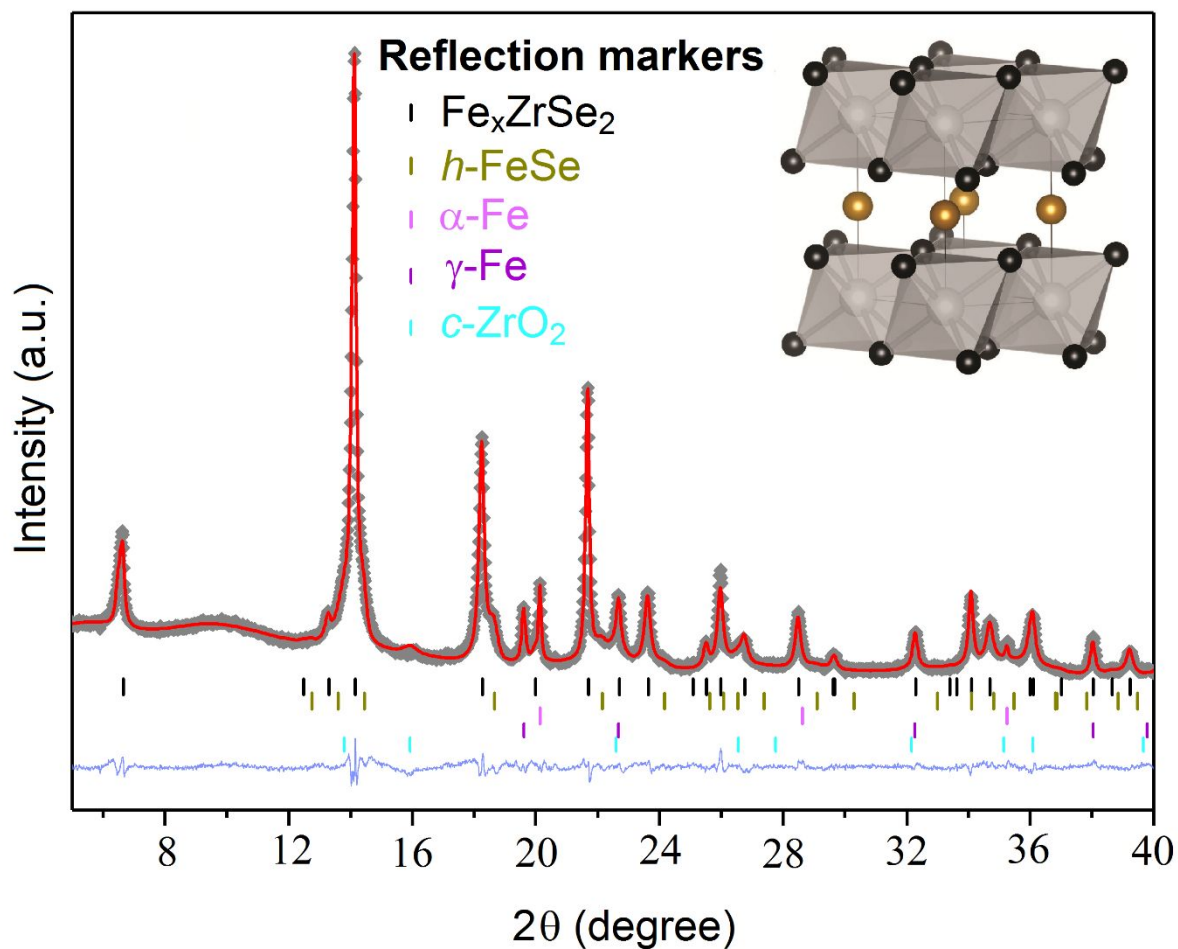


Figure S1. Rietveld refined powder diffraction data (crosses), fit (red line), difference curve (shifted blue line) and reflection markers for all phases (ticks).⁹⁻¹³ Structural analysis was performed using the GSAS package.¹ Embedded in the right corner is an image of the Fe_xZrSe_2 structure drawn from structurally refined PXRD data using VESTA,¹⁴ showing Zr and Se atoms (grey and black spheres) making up triangular layers of ZrSe_2 polyhedra in the *ab* plane, separated by Fe atoms (gold spheres) randomly occupying the octahedral vacancies within the van der Waals gap with a refined occupancy of ~14%.

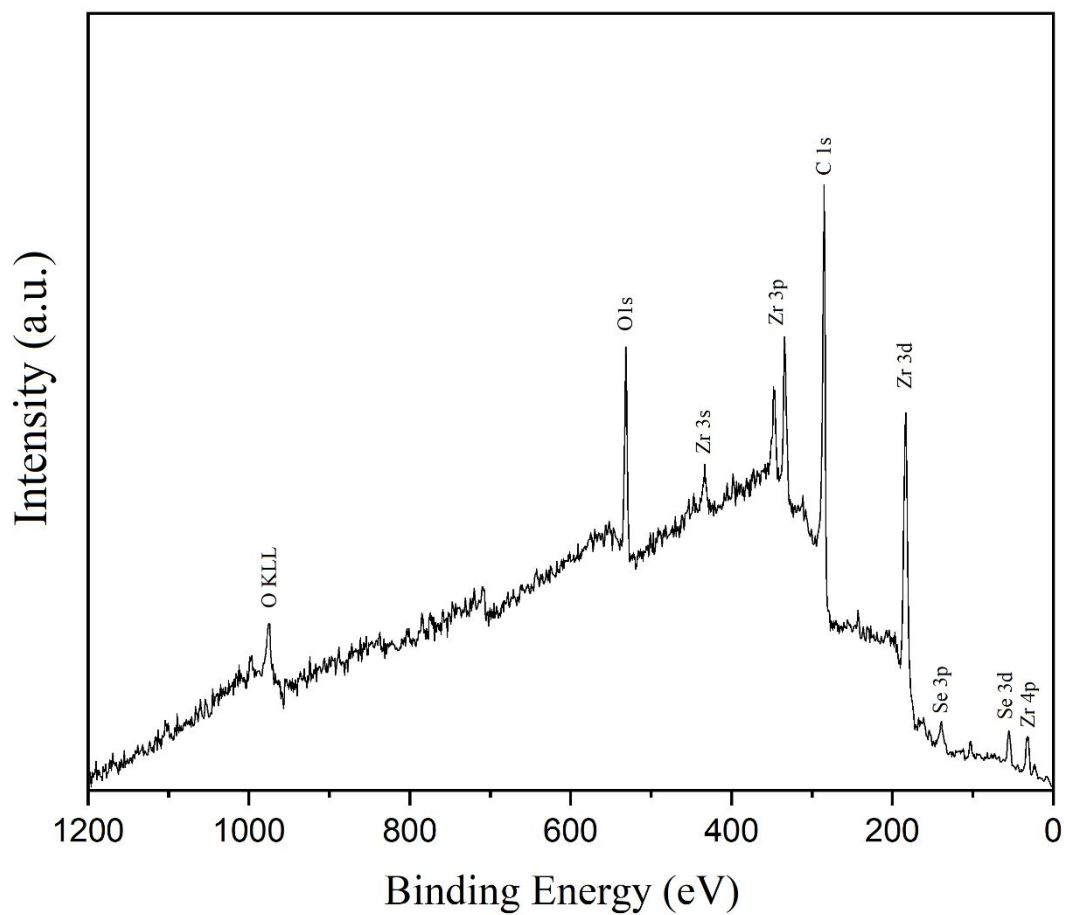


Figure S2. XPS surface survey scan of $\text{Fe}_{0.14}\text{ZrSe}_2$ thin film sample (0 - 1200 eV).

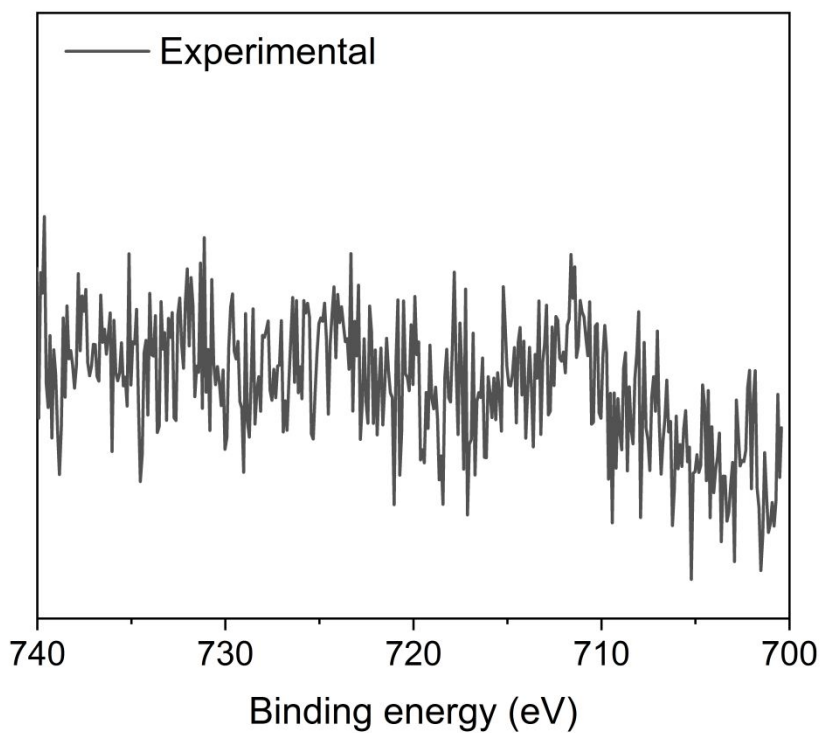


Figure S3. XPS data for the surface of the Fe_xZrSe_2 film showing the Fe 2p region with a low signal to noise ratio.

REFERENCES

- (1) Larson, A. C.; Von Dreele, R. General Structure Analysis System (GSAS). *Los Alamos Natl. Lab. Rep. LAUR* **2004**, 86–748.
- (2) Toby, B. H. EXPGUI, a Graphical User Interface for GSAS. *J. Appl. Crystallogr.* **2001**, *34* (2), 210–213.
- (3) Gleizes, A.; Jeannin, Y. Nonstoichiometry in the ZrSe₂ Phase. *J. Solid State Chem.* **1970**, *1* (2), 180–184.
- (4) Nishimura, E.; Ando, M.; Inada, R.; Hung, M.; Ohashi, N.; Igaki, K. Related Content Electrical Properties of Layered ZrSe₂ Single Crystals Annealed in Selenium Atmosphere. *Jpn. J. Appl. Phys.* **1995**, *34*, 1442.
- (5) Berry, F. J.; Loretto, M. H.; Smith, M. R. Iron-Zirconium Oxides: An Investigation of Structural Transformations by x-Ray Diffraction, Electron Diffraction, and Iron-57 Moessbauer Spectroscopy. *J. Solid State Chem* **1989**, *83* (1), 91–99.
- (6) Related, P. S. Magnetism and Anisotropy of Ultrathin Epitaxial Austenitic Fe-Films. **1989**, 3–6.
- (7) Magnan, H.; Chandris, D.; Villette, B.; Heckmann, O.; Lecante, J. Structure of Thin Metastable Epitaxial Fe Films on Cu(100): Reconstruction and Interface Ordering by Coating. *Phys. Rev. Lett.* **1991**, *67* (7), 859–862.
- (8) Pappas, D. P.; Glesener, J. W.; Harris, V. G.; Idzerda, Y. U.; Krebs, J. J.; Prinz, G. A. Growth of Fcc Fe Films on Diamond. *Appl. Phys. Lett.* **1994**, *64* (1), 28–30.
- (9) Gleizes, A.; Revelli, J.; Ibers, J. A. Structures of a Semiconducting and a Metallic Phase in the Fe_{1-x}ZrSe₂ System. *J. Solid State Chem.* 1976, *17* (4), 363–372.
- (10) Kumar, R. S.; Zhang, Y.; Sinogeikin, S.; Xiao, Y.; Kumar, S.; Chow, P.; Cornelius, A. L.; Chen, C. Crystal and Electronic Structure of FeSe at High Pressure and Low Temperature. *J. Phys. Chem. B* 2010, *114* (39), 12597–12606.
- (11) Gleizes, A.; Revelli, J.; Ibers, J. A. Structures of a Semiconducting and a Metallic Phase in the Fe_{1-x}ZrSe₂ System. *J. Solid State Chem.* 1976, *17* (4), 363–372. [https://doi.org/10.1016/S0022-4596\(76\)80004-7](https://doi.org/10.1016/S0022-4596(76)80004-7).
- (12) Basinski, Z. S.; Hume-Rothery, W.; A. L. Sutton. The Lattice Expansion of Iron. *Proc. R. Soc. Lond. Ser. Math. Phys. Sci.* 1955, 229 (1179), 459–467.
- (13) Martin, U.; Boysen, H.; Frey, F. Neutron Powder Investigation of Tetragonal and Cubic Stabilized Zirconia, TZP and CSZ, at Temperatures up to 1400 K. *Acta Crystallogr. B* 1993, *49* (3), 403–413.
- (14) Momma, K. and Izumi, F. *J. Appl. Crystallogr.*, 2011, *44*, 1272–1276.